CORONAVIRUS

Longitudinal immune profiling reveals key myeloid signatures associated with COVID-19

Elizabeth R. Mann[1,2]*, Madhvi Menon[1]*, Sean Blandin Knight[1,3]*, Joanne E. Konkel[1]*, Christopher Jagger[1], Tovah N. Shaw[1], Siddharth Krishnan[1], Magnus Rattray[4], Andrew Ustianowski[5], Nawar Diar Bakerly[3], Paul Dark[6,7], Graham M. Lord[1], Angela Simpson[6], Timothy Felton[6], Ling-Pei Ho[8]; NIHR Respiratory TRC†, Marc Feldmann[9]; CIRCO‡, John R. Grainger[1§], Tracy Hussell[1*§]

COVID-19 pathogenesis is associated with an exaggerated immune response. However, the specific cellular mediators and inflammatory components driving diverse clinical disease outcomes remain poorly understood. We undertook longitudinal immune profiling on both whole blood and peripheral blood mononuclear cells of hospitalized patients during the peak of the COVID-19 pandemic in the United Kingdom. Here, we report key immune signatures present shortly after hospital admission that were associated with the severity of COVID-19. Immune signatures were related to shifts in neutrophil to T cell ratio, elevated serum IL-6, MCP-1, and IP-10 and modulation of CD14$^+$ monocyte phenotype and function. Modified features of CD14$^+$ monocytes included poor induction of the prostaglandin-producing enzyme, COX-2, and enhanced expression of the cell cycle marker Ki-67. Longitudinal analysis revealed reversion of some immune features back to the healthy median level in patients with a good eventual outcome. These findings identify previously unappreciated alterations in the innate immune compartment of patients with COVID-19 and lend support to the idea that therapeutic strategies targeting release of myeloid cells from bone marrow should be considered in this disease. Moreover, they demonstrate that features of an exaggerated immune response are present early after hospital admission, suggesting that immunomodulating therapies would be most beneficial at early time points.

INTRODUCTION

Severe acute respiratory syndrome coronavirus 2 (SARS-CoV-2) infection can result in the clinical syndrome coronavirus disease 2019 (COVID-19) (*1*) that, to date, has resulted in over 20 million confirmed cases and in excess of 733,000 attributable deaths worldwide. As such, a large number of clinical trials have been established to evaluate antiviral and immunomodulatory strategies aimed at improving clinical outcome for this globally devastating virus.

SARS-CoV-2 is a single-stranded, positive-sense RNA virus that enters cells via human angiotensin-converting enzyme 2 (ACE2) (*2*). Ordinarily, diverse immune mechanisms exist to detect every stage of viral replication and protect the host from viral challenge. Pattern recognition receptors of the innate immune system recognize viral antigen and virus-induced damage, increasing bone marrow hematopoiesis, the release of myeloid cells including neutrophils and monocytes, and the production of a plethora of cytokines and chemokines (*3*). If inflammatory mediator release is not controlled in duration and amplitude, then "emergency hematopoiesis" leads to bystander tissue damage and a cytokine storm that manifests as organ dysfunction. Initial studies suggest that cytokine storm occurs in COVID-19 (*4*). Neutrophilia and lymphopenia [resulting in an increased neutrophil to lymphocyte ratio (NLR)], increased systemic interleukin-6 (IL-6), and C-reactive protein (CRP) correlate with incidence of intensive care admission and mortality (*5*). However, detailed understanding of cellular and molecular inflammatory mediators across the COVID-19 disease trajectory would support the development of better clinical interventions.

We carried out the Coronavirus Immune Response and Clinical Outcomes (CIRCO) study at four hospitals in Greater Manchester, United Kingdom, which was designed to examine the kinetics of the immune response in patients with COVID-19 as well as to identify early indicators of disease severity. Understanding the specific elements and kinetics of the immune response is critical to gain insight into immune phenotypes associated with disease progression, identify potential biomarkers that predict clinical outcomes, and determine at which stage of the disease immunomodulation may be most effective (*4*).

Here, by analyzing fresh blood samples immediately without previous storage, we outline unappreciated immune abnormalities present within patients with COVID-19. Assessment of inflammatory mediators within the blood demonstrated that these immune

[1]Lydia Becker Institute of Immunology and Inflammation, Division of Infection, Immunity & Respiratory Medicine, School of Biological Sciences, Faculty of Biology, Medicine and Health, University of Manchester, Manchester Academic Health Science Centre, Room 2.16, Core Technology Facility, 46 Grafton Street, Manchester M13 9PL, UK. [2]Maternal and Fetal Health Centre, Division of Developmental Biology, School of Medical Sciences, Faculty of Biology, Medicine and Health, University of Manchester, 5th Floor St. Mary's Hospital, Oxford Road, Manchester M13 9WL, UK. [3]Respiratory Department, Salford Royal NHS Foundation Trust, Stott Lane, Salford M6 8HD, UK. [4]Division of Informatics, Imaging and Data Sciences, Faculty of Biology, Medicine and Health, University of Manchester, Manchester M13 9PL, UK. [5]Regional Infectious Diseases Unit, North Manchester General Hospital, Manchester, UK. [6]Division of Infection, Immunity and Respiratory Medicine, Manchester NIHR BRC, Education and Research Centre, Wythenshawe Hospital, Manchester, UK. [7]Intensive Care Department, Salford Royal NHS Foundation Trust, Stott Lane, Salford M6 8HD, UK. [8]MRC Human Immunology Unit, Weatherall Institute of Molecular Medicine, University of Oxford, Oxford, UK. [9]Kennedy Institute of Rheumatology, Botnar Research Centre, Nuffield Department of Orthopedics, Rheumatology and Musculoskeletal Science, Windmill Rd, Headington, Oxford OX3 7LD, UK.
*These authors contributed equally to this work.
†The members of the NIHR Respiratory Translational Research Collaboration (TRC) collaborative group are listed at the end of the Acknowledgments.
‡The members of the Coronavirus Immune Response and Clinical Outcomes (CIRCO) collaborative group can be found at the end of the Acknowledgments.
§Corresponding author. Email: john.grainger-2@manchester.ac.uk (J.R.G.); tracy.hussell@manchester.ac.uk (T.H.)

properties were most dysregulated in patients with severe COVID-19 before admission to intensive care, indicating that immunomodulating therapies should be considered early after admission. Furthermore, our study demonstrated profound alterations in the myeloid cells of patients with COVID-19. Our data demonstrate that monocytes from patients with COVID-19 displayed elevated levels of the cell cycle marker Ki-67 but reduced expression of the prostaglandin-generating enzyme cyclooxygenase-2 (COX-2), with both these features being predominant in patients with severe COVID-19. These findings identify not only possible immune biomarkers for patient stratification but also potential mechanisms of immune dysfunction contributing to the immunopathology of COVID-19.

RESULTS

CIRCO patient clinical characteristics

In total, 73 patients were recruited and 49 were stratified for maximum disease severity (Fig. 1A). Six patients were excluded due to an alternative diagnosis (two patients), indeterminate imaging findings with negative result in the SARS-CoV-2 nasopharyngeal (NP) test (two patients), or diagnosis of a confounding acute illness (two patients). Two patients could not be stratified for disease severity due to insufficient clinical observation data, and a further 16 were not stratified because recruitment occurred more than 7 days after admission. The median time from patient-reported symptom onset to hospital admission was 7 days. The overall median age was 61, and 63% were male. The most frequent comorbidities were diabetes, ischemic heart disease, hypertension, asthma, and chronic obstructive pulmonary disease (Table 1). Most (86%) of the patients tested positive for SARS-CoV-2 via NP reverse transcription polymerase chain reaction (RT-PCR). In 14% of patients, symptoms and radiographic features were highly suggestive of COVID-19, but NP test was negative for the virus, and thus, a clinical diagnosis was made; these patients are indicated in all graphs (white triangles). Patient disease severity was defined as mild (less than 28% FiO_2), moderate (28 to 60% FiO_2), or severe (above 60% FiO_2, or admission to intensive care) (Fig. 1B). Death occurred in 50% of severe cases of COVID-19, and only 1 of the 10 patients with severe disease was categorized as severe upon admission.

Broad shifts in the innate and adaptive immune compartments in patients with COVID-19

On the basis of blood cell counts by the hospital laboratory at admission, no significant differences in total white blood cells, neutrophils, monocytes, or lymphocytes were observed between groups of patients with COVID-19 that went on to progress to mild, moderate, or severe disease (fig. S1A). However, as reported previously (*6*, *7*), a trend was evident toward a higher NLR at hospital admission in those patients whose outcome eventually was severe (fig. S1B). This suggested that a more in-depth immune profiling could aid in patient stratification before escalation of the disease.

Thus, we further explored alterations in the innate and adaptive immune compartments using high-dimensional flow cytometry on white blood cells from freshly lysed whole blood (see fig. S1C for gating strategy). Initially, we examined the first blood sample taken at the time of patient recruitment to the study (this was typically 2 to 3 days after hospital admission and was not greater than 7 days). At this recruitment time point, alterations to the characteristics and relative abundance of diverse immune cell types were observed. Uniform manifold approximation and projection (UMAP) visualization outlined alterations between patients and healthy controls in the characteristics of neutrophils and monocytes, marked increases in the frequency of neutrophils, and decreased T cells, B cells, and basophils. Cellular changes were exaggerated with disease severity (Fig. 2A). In a subset of infected individuals, $CD16^{low}$ granulocytes were present (Fig. 2A); these cells can be associated with altered immune cell output from the bone marrow (*8*). This global picture of alterations to innate and adaptive immune cells was confirmed by manual flow cytometric gating (Fig. 2B and fig. S1, C and D). In addition to these alterations, examining cell frequencies within isolated peripheral blood mononuclear cells (PBMCs) revealed a decrease in the frequency of plasmacytoid dendritic cells in patients with COVID-19, which was enhanced with elevated disease severity (fig. S1E). There were no changes observed in frequencies of $CD56^{+}$ natural killer (NK) cells (fig. S1E).

Given the marked alterations in neutrophil and T cell frequencies at the time of recruitment (Fig. 2B), we next examined their profile longitudinally over the course of hospitalization. To do this, we used the first day of patient-reported

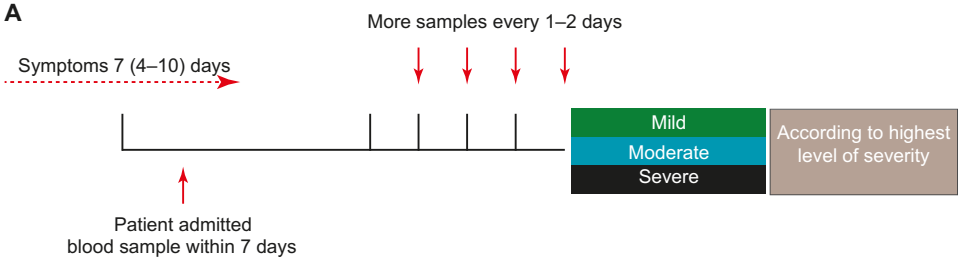

B

Severity score	Criteria
Mild	• <3 liters/min or <28% supplemental oxygen required to maintain target oxygen saturations • Managed in a ward-based environment
Moderate	• <10 liters/min or <60% supplemental oxygen required to maintain target oxygen saturations • Managed in a ward-based environment • Chronic NIV or CPAP (home use) or acute NIV for COPD
Severe	Any of: • >10 liters/min or 60% supplemental oxygen required to maintain target oxygen saturations • Use of acute NIV (not for COPD) • Managed in ICU/invasive ventilation

Fig. 1. Patient recruitment and categorization. (**A**) Patients were recruited to the study as close to admission as possible and within 7 days. Peripheral blood samples were collected on recruitment and at intervals thereafter. Samples were analyzed immediately, and results were stratified based on their ultimate disease severity. (**B**) Criteria for patient stratification. NIV, noninvasive ventilation; CPAP, continuous positive airway pressure; COPD, chronic obstructive pulmonary disease.

Table 1. Clinical characteristics. Data are listed as median (IQR)[m], where *m* is the number of missing data points, *n* (%), or *n*/*N* (%), where *N* is the total number with available data. Representative participants from each severity cohort were used in cross-sectional or longitudinal analysis.

	All patients (49)	Mild (18)	Moderate (21)	Severe (10)
Age	61 (51–71)	61.5 (45–72.5)	59 (51–68)	66 (52–72.5)
Sex				
Male	31 (63.3%)	11 (61.1%)	13 (62%)	7 (70%)
Female	18 (36.7%)	7 (38.9%)	8 (38%)	3 (30%)
Body mass index	27.5 (24.9–30)[4]	27.1 (23.6–30)[1]	28.3 (25.7–30)[2]	26.5 (24.9–30.4)[1]
Comorbidity				
Diabetes	8/49 (16.3%)	3/18 (16.7%)	2/21 (9.5%)	3/10 (30%)
Ischemic heart disease	5/49 (10.2%)	2/18 (11.1%)	1/21 (4.8%)	2/10 (20%)
Hypertension	14/49 (28.6%)	5/18 (27.8%)	7/21 (33.3%)	2/10 (20%)
Chronic obstructive pulmonary disease	9/49 (18.4%)	4/18 (22.2%)	4/21 (19.1%)	1/10 (10%)
Asthma	5/49 (10.2%)	2/18 (11.1%)	3/21 (14.3%)	0/10 (0%)
Malignancy	3/49 (6.1%)	0/18 (0%)	1/21 (4.8%)	2/10 (20%)
Presentation				
Illness onset to admission (days)	7 (4–10)[4]	7 (4–8)[1]	7.5 (2.8–10.8)[3]	5.5 (4–9.5)
Dyspnea	29/41 (70.7%)	8/16 (50%)	14/16 (87.5%)	7/9 (77.8%)
Cough	30/41 (73.2%)	11/16 (68.8%)	12/16 (75%)	7/9 (77.8%)
Fever	28/41 (68.3%)	10/16 (62.5%)	9/16 (56.3%)	9/9 (100%)
Diarrhea/vomiting	14/41 (34.2%)	3/16 (18.8%)	7/16 (43.8%)	4/9 (44.4%)
Myalgia	10/40 (25%)	4/15 (26.7%)	3/16 (18.8%)	3/9 (33.3%)
Fatigue	10/38 (26.3%)	3/14 (21.4%)	5/15 (33.3%)	2/9 (22.2%)
Day recruited	2 (2–3)	3 (2–4.5)	2 (2–3)	2 (2–3)
Number of time points	2 (1–4)	2 (1–2)	3 (2–3)	4.5 (2–5)
Respiratory rate*	20 (18–25)[10]	20 (17–24)[5]	21 (18–26)[3]	21.5 (17.8–24)[2]
Temperature*	37.5 (36.9–38.4)[10]	37.1 (36.5–37.4)[5]	37.7 (37.1–38.8)[3]	38 (37.7–39.2)[2]
Systolic blood pressure*	125 (117–136)[10]	122 (117–126)[5]	126 (118–136)[3]	137.5 (114.5–156.3)[2]
Chest radiograph findings				
Bilateral opacification	41/47 (87.2%)	11/16 (68.8%)	20/21 (95.2%)	10/10 (100%)
Unilateral opacification	3/47 (6.4%)	2/16 (12.5%)	1/21 (4.8%)	0/10 (0%)
No abnormality	3/47 (6.4%)	3/16 (18.8%)	0/21 (0%)	0/10 (0%)
COVID nasopharyngeal test				
Positive	42 (86%)	15 (83.3%)	18 (85.7%)	9 (90%)
Negative	7 (14%)	3 (16.7%)	3 (14.3%)	1 (10%)
Differential full blood count at admission				
White blood cell count ($\times 10^9$/liter)	6.9 (5.7–9.8)	6.7 (4.7–7.5)	7.1 (6.3–10)	7.3 (5.7–10)
Lymphocytes ($\times 10^9$/liter)	1.1 (0.8–1.4)	1.2 (0.8–1.3)	1.3 (0.8–1.5)	0.9 (0.8–1.1)
Neutrophils ($\times 10^9$/liter)	5.1 (3.8–7.4)	4.7 (3.2–5.7)	5.3 (4.5–7.7)	6.3 (4.2–8.6)
Monocytes ($\times 10^9$/liter)	0.4 (0.2–0.7)	0.4 (0.2–0.6)	0.5 (0.3–0.7)	0.3 (0.2–0.5)
Platelets ($\times 10^9$/liter)	244 (188–367)[2]	241 (188–316)[2]	269 (195–366)	204 (155–412)
Highest acute-phase response/liver function tests				
CRP (mg/liter)	127 (75–226)	88 (38–166)	120 (75–201)	269 (244–296)
Alanine aminotransferase (U/liter)	48 (27–87)[16]	57 (28–75)[9]	35 (25–79)[5]	49 (37–105)[2]

continued on next page

	All patients (49)	Mild (18)	Moderate (21)	Severe (10)
Alkaline phosphatase (U/liter)	78 (63–96)[16]	79 (63–82)[9]	72 (63–90)[5]	110 (71–172)[2]
Bilirubin (μM)	11 (7–15)[16]	10 (8–14)[9]	9 (7–13)[5]	13 (10–21)[2]
Complications				
Pulmonary embolism	5/49 (10.2%)	1/18 (5.6%)	4/21 (19.1%)	0/10 (0%)
Acute kidney injury	3/49 (6.1%)	0/18 (0%)	2/21 (9.5%)	1/10 (10%)
Mortality	6/49 (12.2%)	1/18 (5.6%)	0/21 (0%)	5/10 (50%)

*Admission observations.

symptom onset as a common reference point to align patient disease trajectories. This revealed that, in most of the patients, irrespective of final severity, neutrophil frequencies, although initially extremely high, decreased before hospital discharge, while T cell frequencies reciprocally increased (Fig. 2, C and D). In contrast, $CD14^+$ monocytes and B cells showed no obvious trends during the hospital stay (Fig. 2, C and D). These data highlight the importance of examining NLR in patients with COVID-19 (*6*, *7*) but, along with other studies (*9*), indicate that assessment of neutrophil to T cell ratio may provide a more stringent disease insight. In two severe patients with poor outcome, T cell frequencies were extremely low and neutrophil frequencies were high even after entry into an intensive care unit (ICU) (Fig. 2C, white and pink crossed squares, and Fig. 2D, red triangles), indicating that rebalancing of neutrophil to T cell ratio is crucial to recovery.

Defined soluble mediators are associated with severe disease

Broad changes in circulating immune cells in other viral infections are associated with alterations to circulating inflammatory mediators, such as cytokines and chemokines. These are potent modifiers of bone marrow output, immune cell survival, and cell recruitment to the inflamed lung. We used multiplex bead array to assess soluble inflammatory mediators in serum from patients at recruitment to the study. Of the 13 mediators analyzed in serum, IL-6, IL-10, monocyte chemoattractant protein-1 (MCP-1), and interferon-γ (IFN-γ)–induced protein 10 (IP-10) were significantly increased in patients with COVID-19 and tracked with disease severity (fig. S2A). No significant changes in other cytokines or chemokines measured, including IFN-γ, IL-1β, IL-8, and tumor necrosis factor–α (TNF-α), were observed in patients with COVID-19 (fig. S2B).

Longitudinal analysis (examined as above from the day of reported disease onset) of IL-6, MCP-1, and IP-10 in mild and severe patients revealed that the highest levels of these cytokines and chemokines occurred early in the disease trajectory at recruitment to the study (fig. S2C). There was a significant decrease in IL-6 and IP-10 in patients upon recovery (fig. S2D). There was a marked reduction in IL-6, IP-10, and MCP-1 upon admission of severe patients into ICU from the ward (fig. S2E), although this finding is based on just three patients. This may be due to the treatment modalities used in intensive care, such as sedation, that can have immunomodulatory effects (*10*) and will be important to investigate further. The patient whose health declined rapidly after admission, and ultimately died from the disease, displayed a marked rebound in IL-6 and MCP-1 levels after 2 days on ICU (fig. S2, D and E, red triangles).

Activation of adaptive immune cells in patients with COVID-19

To build on our basic assessment of cell populations outlined in Fig. 2, we next investigated alterations to specific T and B cell populations by flow cytometrically analyzing isolated PBMCs. Within the T cell compartment, we noted no marked alterations in $CD4^+$ or $CD8^+$ T cell frequencies (Fig. 3, A and B). However, a slight decrease in $CD4^+$ T cells was observed in patients with severe COVID-19 (Fig. 3B). Both T cell subsets showed signs of activation in patients with COVID-19, and this was more apparent in $CD8^+$ T cells. The degree of T cell activation did not track with disease severity and was highly variable among patients (fig. S3, A to D). Despite this, patients with COVID-19 exhibited decreased frequencies of naive but elevated frequencies of effector TEMRA and $HLA\text{-}DR^+CD38^+CD8^+$ T cells (fig. S3, A to C). $CD8^+$ T cell subsets remained stable over the hospitalized disease course (fig. S3E).

In 34 of 43 patients with COVID-19, higher perforin expression was observed in $CD8^+$ T cells compared with healthy individuals (Fig. 3C and fig. S3F), implying that $CD8^+$ T cells in patients with COVID-19 had activated a cytotoxic program. Perforin expression in $CD8^+$ T cells did not track with disease severity (Fig. 3D), but a positive correlation was observed between the frequency of $perforin^+CD8^+$ T cells and clinical measurements of the inflammatory marker CRP (Fig. 3E). This indicates that increased frequencies of circulating $perforin^+CD8^+$ T cells are more prevalent in highly inflamed patients. However, $perforin^+CD8^+$ T cells were found to increase over time in mild and most moderate COVID-19 patients, with highest levels immediately before discharge (fig. S3, G and H), suggesting that the higher frequencies seen in severe patients are not necessarily detrimental. Overall, these data demonstrate heterogeneous T cell activation in patients with COVID-19, but a consistent cytotoxic profile in the $CD8^+$ T cell compartment.

Similar to the trend in whole blood (Fig. 2B), B cell frequency was reduced in PBMCs of patients with COVID-19. Decreases were particularly notable in severe patients compared with those with mild and moderate disease (Fig. 3F) and persisted with time (fig. S4A). Although reduced in frequency, B cells displayed increased expression of Ki-67 (indicative of proliferation), which positively correlated with CRP levels (Fig. 3G). When examining B cell subsets, we observed an expansion of antibody-secreting plasmablasts ($CD27^{hi}CD38^{hi}CD24^-$) that positively correlated with immunoglobulin G (IgG) expression by B cells (Fig. 3, H and I). Furthermore, we observed a decrease in unswitched memory ($CD27^+IgD^+IgM^+$) B cells but no global differences in frequencies of other B cell subsets (fig. S4B). The differences in B cell subsets did not track with

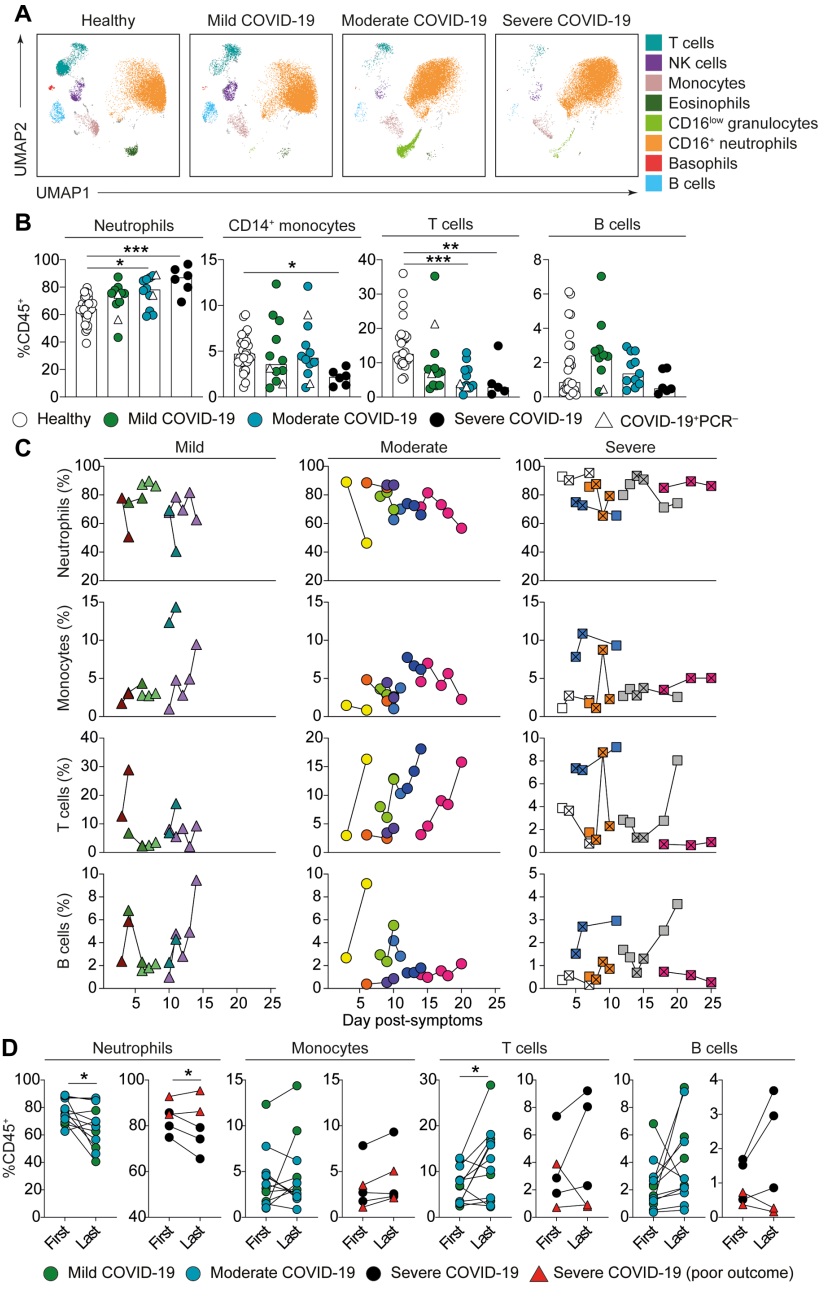

Fig. 2. Whole blood immune profile of patients with COVID-19. (**A**) UMAP of flow cytometry panel broadly visualizing white cells in whole blood. Representative images for healthy individuals and mild, moderate, and severe patients are shown. Key indicates cells identified on the image. (**B**) Graphs show neutrophil ($CD16^+CD11b^{hi}$), $CD14^+$ monocyte, $CD3^+$ T cell, and $CD19^+$ B cell frequencies in whole blood samples of healthy individuals ($n = 28$) and recruitment samples from COVID-19 patients with mild ($n = 12$), moderate ($n = 13$), and severe ($n = 6$) disease. (**C**) Longitudinal time course of (top row) neutrophils ($CD16^+CD11b^{hi}$), (second row) $CD14^+$ monocytes, (third row) $CD3^+$ T cells, and (bottom row) B cells segregated by disease severity. Individual patients are shown as different colors and shapes, with lines connecting data from the same patient. Crossed squares for severe patients are time points in ICU. *X*-axis values represent the number of days since reported onset of symptoms. (**D**) Graphs showing frequencies of neutrophils ($CD16^+CD11b^{hi}$), monocytes, T cells, and B cells at the first and last time points in (left) mild/moderate patients (green and blue circles) and (right) severe patients (black circles). Red triangles represent severe patients that had poor outcome (deceased or long-term ICU) and are not included in the statistical test. Graphs show individual patient data, with the bar representing median values. In all graphs, open triangles represent SARS-CoV-2 PCR-negative patients. (B) Kruskal-Wallis with Dunn's post hoc test: Neutrophils, T cells, and B cells; one-way ANOVA with Holm-Sidak post hoc test: $CD14^+$ monocytes. (D) Paired *t* test: All except monocyte graph detailing mild and moderate patients, which was tested using Wilcoxon matched-pairs signed-rank test. $^*P < 0.05$, $^{**}P < 0.01$, $^{***}P < 0.001$, $^{****}P < 0.0001$.

disease severity (fig. S4C). The only subpopulation of B cells markedly expanded in patients with severe COVID-19, compared with patients with mild and moderate disease, was double-negative (DN) B cells ($CD27^-IgD^-$) (Fig. 3J). This subset was relatively stable throughout patient hospitalization and associated with a worse disease trajectory (fig. S4D). DN B cells have previously been associated with an exhausted phenotype in patients with HIV (*11*), suggesting that patients with severe COVID-19 may have an impaired capacity to generate an effective B cell response.

Altered monocyte phenotype and function is a feature of COVID-19

COVID-19 research to date has primarily focused on T and B cells, although recent publications have highlighted alterations to monocyte phenotype (*12*). Monocytes can be important contributors to inflammatory disease directly or via differentiation to macrophages and dendritic cells (*13*, *14*). When released into the blood stream, monocytes will be affected by circulating cytokines and chemokines, including MCP-1, which we define as raised early in COVID-19 sera (fig. S2A). In patients with COVID-19, we observed an expansion of intermediate $CD14^+CD16^+$ monocytes that tended to be highest in patients with a mild disease outcome (fig. S5, A and B). Enhanced expression of CD64, the high-affinity Fc receptor for monomeric IgG (FcγRI), was apparent on classical $CD14^+$ monocytes (Fig. 4A) and again was most evident in mild disease.

We next examined monocyte activation by stimulating with lipopolysaccharide (LPS); stimulation frequencies of viable cells were high (greater than 90%) and similar in patients with COVID-19 and healthy controls. After stratification for final disease severity, TNF-α was enhanced in patients with mild disease (Fig. 4B and fig. S5C). In contrast, IL-1β production was lower in monocytes from patients with COVID-19 compared with monocytes from healthy individuals (fig. S5D), although this was not related to disease severity. These data highlight that monocytes from patients with COVID-19 exhibit a modified cytokine profile upon activation. As well as cytokines, monocytes are major

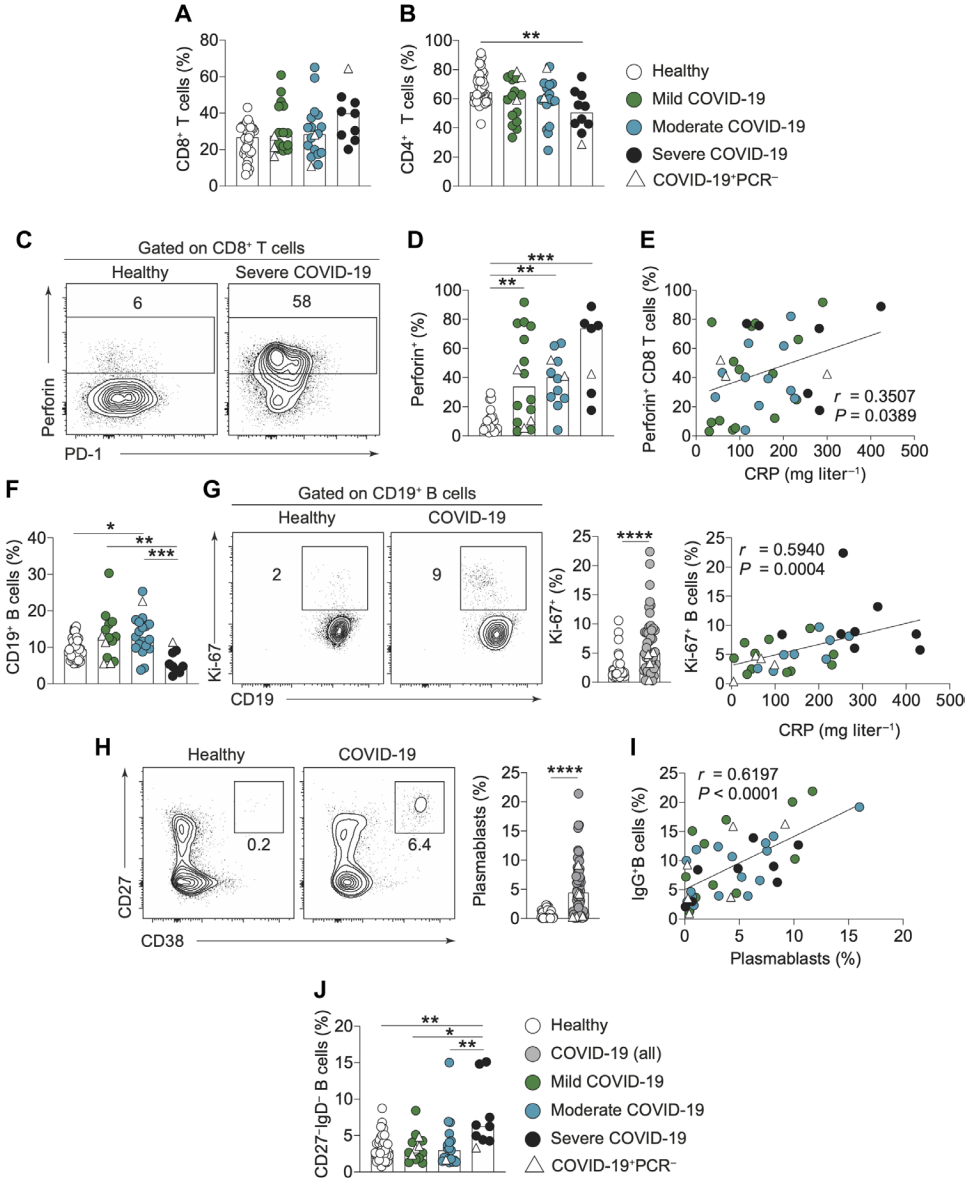

Fig. 3. Altered phenotype of T and B cells in patients with COVID-19. (**A** and **B**) Graphs show frequencies of (A) $CD8^+$ and (B) $CD4^+$ T cells in freshly isolated PBMCs of healthy individuals ($n = 36$) and recruitment samples from COVID-19 patients with mild ($n = 17$), moderate ($n = 18$), and severe ($n = 9$ to 10) disease. (**C** and **D**) Representative flow cytometry plots and graph showing frequency of $CD8^+$ T cells that are positive for perforin in healthy individuals ($n = 21$) and COVID-19 patients with mild ($n = 16$), moderate ($n = 12$), and severe ($n = 7$) disease. (**E**) Graph showing correlation of perforin$^+$$CD8^+$ T cell frequency with CRP in patients with COVID-19. (**F**) Graphs show frequencies of $CD19^+$ B cells in freshly isolated PBMCs of healthy individuals ($n = 43$) and recruitment samples from COVID-19 patients with mild ($n = 14$), moderate ($n = 19$), and severe ($n = 9$) disease. (**G**) Representative flow cytometry plots and cumulative data show Ki-67 expression by B cells in healthy individuals ($n = 39$) and patients with COVID-19 ($n = 45$). Correlation graph shows correlation of Ki-67$^+$ B cells with CRP. (**H**) Representative flow cytometry plots and cumulative data show frequency of $CD27^{hi}CD38^{hi}$ plasmablasts in healthy individuals ($n = 42$) and in patients with COVID-19 ($n = 66$). (**I**) Correlation graph shows correlation of plasmablasts and IgG^+ B cell frequencies. (**J**) Graph shows frequencies of DN ($CD27^-IgD^-$) B cells in freshly prepared PBMCs of healthy individuals ($n = 42$) and recruitment samples from COVID-19 patients with mild ($n = 14$), moderate ($n = 19$), and severe ($n = 9$) disease. Graphs show individual patient data, with the bar representing median values. In all graphs, open triangles represent SARS-CoV-2 PCR-negative patients. Mann-Whitney *U* test (G and H), Kruskal-Wallis with Dunn's post hoc test (A, D, F, and J), one-way ANOVA with Holm-Sidak post hoc test (B), and Spearman ranked coefficient correlation test (E, G, and I). $^*P < 0.05$, $^{**}P < 0.01$, $^{***}P < 0.001$, $^{****}P < 0.0001$.

producers of lipid mediators, such as prostaglandins (*15*), and so, we also examined COX-2 expression (a rate-limiting enzyme in prostaglandin synthesis). In LPS-stimulated monocytes, a reduction in COX-2 was evident in all patients with COVID-19 and was most apparent in those with severe disease (Fig. 4, C to E). Accordingly, expression of COX-2 in stimulated monocytes was inversely correlated to systemic levels of the cytokine MCP-1 (fig. S5E), which were highest in patients with severe COVID-19 (fig. S2A).

One possible reason that monocytes in patients with COVID-19 display altered functionality in the periphery is due to inflammation-induced emergency myelopoiesis (*3*). This process occurs during infection where hematopoietic stem cells and myeloid progenitors expand in the bone marrow to provide more cells to combat viral infection. However, if egress is too fast, then monocytes exit in an altered state. For example, unusually high expression of the cell cycle marker Ki-67 is observed in peripheral monocytes during H1N1 influenza (*16*) and Ebola virus (*17*) infection. We therefore investigated expression of the proliferation marker Ki-67 in COVID-19. A marked increase in Ki-67$^+$ monocytes (<5% in monocytes from most healthy controls) was evident in patients with COVID-19 but was most marked in patients with severe disease (Fig. 4, F and G). Ki-67 expression strongly correlated with CRP levels (Fig. 4H), and with systemic levels of the cytokines IL-6, MCP-1, IP-10, and IL-10 (fig. S5F), cytokines that were enhanced in patients with COVID-19 and tracked with severity (fig. S2A). Enhancement of Ki-67 expression was also observed in unstimulated monocytes from patients with COVID-19 (fig. S5G).

We next assessed how monocyte alterations varied over the patients' hospital stay and noted that patients with mild COVID-19 had consistently higher TNF-α and COX-2 expression in LPS-activated monocytes compared with patients with severe disease (Fig. 4, I and J). COX-2 remained low in severe patients throughout intensive care, but levels were restored upon recovery in mild patients (Fig. 4L). IL-1β was consistently low over time in both severity groups, with

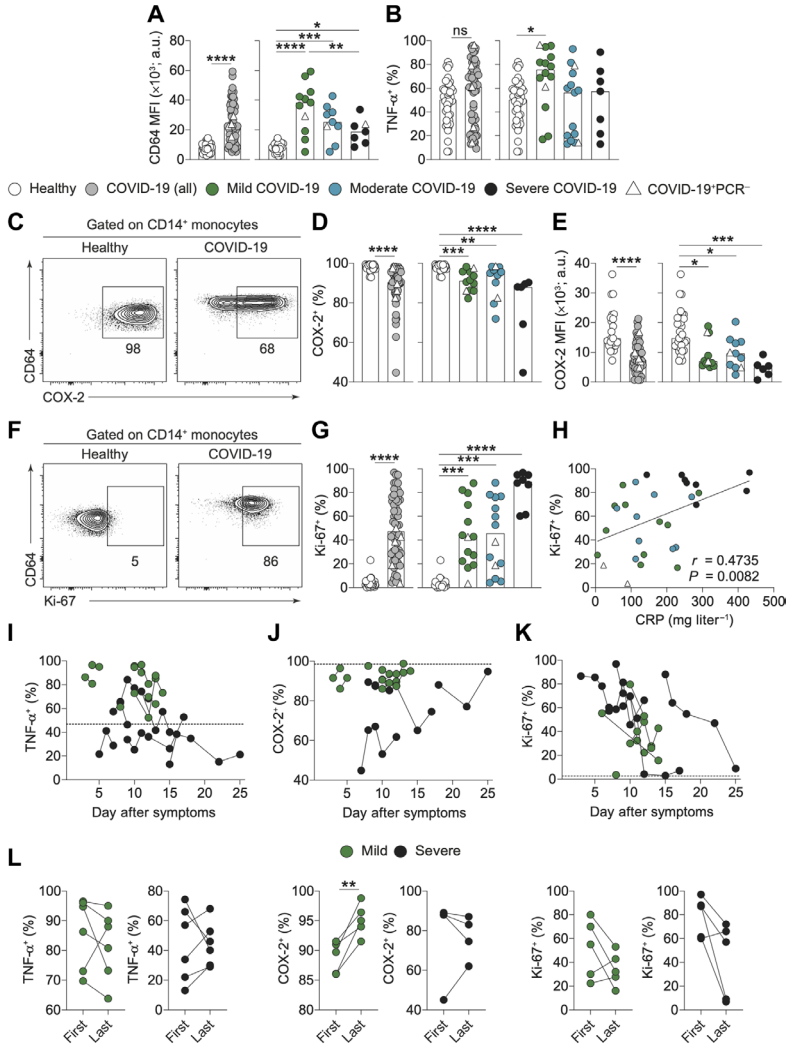

Fig. 4. Dysregulation of circulating monocytes in COVID-19. (**A**) Graphs show levels of CD64 expression as assessed by mean fluorescence intensity (MFI) on CD14$^+$ classical monocytes in freshly prepared PBMCs of healthy individuals ($n = 25$) and recruitment samples from all patients with COVID-19 ($n = 58$). Patients with COVID-19 were also stratified into mild ($n = 12$), moderate ($n = 10$), and severe ($n = 8$) disease. a.u., arbitrary units. (**B**) Graphs show frequencies of TNF-α$^+$ CD14$^+$ monocytes after LPS stimulation of freshly prepared PBMCs from healthy individuals ($n = 41$) and patients with COVID-19 ($n = 59$). Patients with COVID-19 were also stratified into mild ($n = 14$), moderate ($n = 15$), and severe ($n = 7$) disease. (**C**) Representative fluorescence-activated cell sorting (FACS) plots demonstrating intracellular COX-2 expression by CD14$^+$ monocytes from healthy individuals and patients with COVID-19. (**D** and **E**) Graphs showing (D) frequencies of COX-2$^+$ CD14$^+$ monocytes and (E) COX-2 expression level as determined by MFI in CD14$^+$ monocytes after LPS stimulation of freshly prepared PBMCs from healthy individuals ($n = 33$) and total COVID-19 patients ($n = 51$). Patients with COVID-19 were also stratified into mild ($n = 12$), moderate ($n = 11$), and severe ($n = 6$) disease. (**F**) Representative FACS plots demonstrating intracellular Ki-67 staining by CD14$^+$ monocytes. (**G**) Graphs show frequencies of Ki-67$^+$ CD14$^+$ monocytes after LPS stimulation of freshly prepared PBMCs from healthy individuals ($n = 37$) and total COVID-19 patients ($n = 60$). Patients with COVID-19 were also stratified into mild ($n = 14$), moderate ($n = 14$), and severe ($n = 8$) disease. (**H**) Correlation of Ki-67 (percentage of monocytes expressing Ki-67) with CRP in patients with COVID-19. (**I** to **K**) Longitudinal time course of frequencies of CD14$^+$ monocytes that are positive for (I) TNF-α, (J) COX-2, and (K) Ki-67 after LPS stimulation in mild (green shapes, $n = 6$ to 7) and severe (black shapes, $n = 4$ to 6) COVID-19 patients, with lines connecting data from the same patient. On all graphs, *x*-axis values represent the number of days since onset of symptoms and the dotted line represents the median value from healthy individuals. (**L**) Graphs showing frequencies of monocytes that are TNF-α$^+$, COX-2, and Ki-67$^+$ after LPS stimulation at the first and last time points in (left) mild patients (green circles) and (right) severe patients (black circles). Graphs show individual patient data, with the bar representing median values. In all graphs, open triangles represent SARS-CoV-2 PCR-negative patients. Mann-Whitney *U* test (A, B, D, E, and G), Kruskal-Wallis with Dunn's post hoc test (B, D, E, and G), one-way ANOVA with Holm-Sidak post hoc test (A), Spearman ranked coefficient correlation test (H), and paired *t* test (L). *$P < 0.05$, **$P < 0.01$, ***$P < 0.001$, ****$P < 0.0001$.

no significant differences in monocyte production of IL-1β between the first and last measured time points from mild or severe patients (fig. S5H). Ki-67 expression, however, was highest at recruitment and decreased in patients (back down to levels seen in healthy controls) during the progression of disease, independent of severity category or final outcome (Fig. 4, K and L). Thus, defined alterations to monocyte function, specifically to TNF-α and COX-2, are maintained across the disease time course and levels of expression are associated with severity. Together, these findings highlight alterations to monocyte phenotype and function as key features of disease progression and severity in COVID-19.

DISCUSSION

Respiratory viruses continue to cause devastating global disease. This detailed, prospective, observational analysis of patients with COVID-19 of varying severity and outcome, in real time, has revealed specific immunological features that track with disease severity, providing important information concerning pathogenesis that should influence clinical trials and therapeutics. Of particular importance, increased expression of the cell cycle marker Ki-67 in blood monocytes, reduced expression of COX-2, and a high neutrophil to T cell ratio are early predictors of disease severity that could be used to stratify patients upon admission for therapeutics. Critically, most of the aberrant immune parameters studied reverted in patients with good outcome. Unexpectedly, multiple aspects of inflammation that were high upon admission diminished as patients progressed in severity and were admitted to intensive care. In particular, levels of IP-10 and Ki-67 expression by monocytes were reduced after admission to intensive care, even in patients who did not recover. These data indicate that treating patients early after hospitalization is likely to be most beneficial, while cytokine levels and immune functions are disrupted.

Although other studies have focused on defects in adaptive immunity in COVID-19 pathogenesis (*18*), we demonstrate here considerable abnormalities in the innate immune system, in particular

within myeloid cells. Profound neutrophilia exists in severe COVID-19, supportive of a role for neutrophils in acute respiratory distress syndrome (*19*, *20*) and in line with the excess neutrophils seen in the autopsied lungs of patients that died from COVID-19 (*21*). Neutrophils assist in the clearance of pathogens through phagocytosis and oxidative burst and by liberating traps [neutrophil extracellular traps (NETs)] that capture pathogens. The latter two functions, however, can also promote inflammation and are associated with many of the features seen in COVID-19 (*22*). Elevated neutrophil products have been identified in the sera of patients with COVID-19 and correlate with clinical parameters such as CRP, D-dimer, and lactate dehydrogenase (*23*).

Altered monocyte phenotypes were also seen in patients with COVID-19, with patient blood monocytes expressing the cell cycle marker Ki-67 (up to 98%), a feature not observed in healthy individuals. This likely represents either early or enhanced release of monocytes from the bone marrow due to systemic inflammatory signals and is similar to that described in pandemic H1N1 influenza (*16*) and Ebola virus infections (*17*). Equally remarkable was the reduced expression of COX-2 in monocytes in patients with severe disease, which was evident across their disease trajectory. COX-2 facilitates the production of prostanoids including prostaglandin E_2 (PGE_2), and other viruses are known to target this pathway to enhance viral replication (*24*). However, its reduction in monocytes in response to viral lung infection has not previously been reported. Reduced COX-2 alongside high IL-6 and IP-10, as seen here in patients with severe COVID-19, is an immune profile associated with pathology in idiopathic pulmonary fibrosis (*25*). Therefore, our data indicate a possible fibrotic signature in patients with severe disease, supporting studies observing an unusual pattern of fibrosis in the lungs of patients with COVID-19.

Our data concur with several features of COVID-19 studied in Wuhan, China, as well as with more recent studies from across the globe (*26*, *27*) and are also corroborated by single-cell RNA sequencing of bronchoalveolar lavage cells at a single time point (*28*). Similarities include elevated CRP and IL-6 in patients at the time of hospitalization who eventually died (*29*) and increased IP-10 in those who later developed severe disease (*30*). IP-10 is an interferon-inducible chemokine that facilitates directed migration of many immune cells (*31*) and is elevated in other coronavirus infections including MERS-CoV and SARS-CoV (*32*), as well as in Influenza virus of swine origin (H1N1) (*33*, *34*). The heightened levels of MCP-1 upon admission further indicate dysregulation of monocyte function and migration in patients with severe disease. IL-6, IP-10, and MCP-1 levels are generally the highest around the time of hospital admission but are reduced rapidly as patients are admitted to intensive care, which may well signify exhaustion of the immune cells producing these mediators.

Examining cells of the adaptive immune system, we identified lymphopenia, which is now a well-established hallmark of patients with COVID-19 (*35*–*38*). Despite this being a key feature of COVID-19, the drivers of loss of T and B cell numbers in peripheral blood remain obscure and could equally reflect either cell death and/or elevated trafficking to the site of inflammation. Focusing on T cells, the phenotype and function of circulating T cells remain an issue with conflicting reports within the literature. Consistent with previous reports, our data show modest increases in T cell activation (*27*, *39*, *40*), primarily driven by a substantial heterogeneity between patients. Despite this, the frequencies of T cells with activated phenotypes remained stable across the disease trajectory, implying that most changes to these adaptive mediators could have occurred before hospitalization. Our data highlight activation of a cytotoxic program in $CD8^+$ T cells, evidenced by perforin expression, which would support effective viral clearance that has previously been suggested (*41*). Focusing on B cells, patients with severe COVID-19 displayed a marked expansion of $CD27^-IgD^-$ DN B cells. This is in agreement with a recent study reporting lupus-like hallmarks of extrafollicular B cell activation in critically unwell COVID-19 patients (*42*). DN B cells are also associated with immune senescence as a result of excessive immune activation, and an exhausted phenotype is observed in patients with HIV (*11*). Further studies evaluating the functional capacity of expanded DN B cells will be critical to understand their contribution to severe COVID-19.

There are, of course, limitations to any study of samples during a viral pandemic for which there is no vaccine. However, we believe that these do not diminish the importance of the major findings from our study. A longitudinal analysis in real time for phenotypic, functional, and soluble markers naturally limits the number of patients interrogated. In-depth analysis of smaller cohorts, however, is necessary to gain insight into mechanism and is of interest to the pharmaceutical industry. It takes time to recruit the appropriate number of control subjects of the approximate gender and age of patients with COVID and also with the span of comorbidities associated with the greatest risk from SARS-CoV-2. Most of our controls were drawn from frontline workers, who produced similar results to each other. The only other potential limitation is that patients may not accurately define the onset of symptoms. As data are plotted per patient, however, this does not affect the interpretation of the results.

There are clinical implications of our data. Using nonsteroidal anti-inflammatory drugs remains controversial (*43*), and our study would suggest that they may not be desirable, as this may compound the already low COX-2 (*44*). Because most of the pathogenic mechanisms involve myeloid cells, neutrophils, and monocytes, it would be advantageous to reduce their influx to the lung once lung pathology is established. Relevant strategies include inhibition of the complement anaphylatoxin C5a (*45*) or IL-8 (CXCL8), which are strong chemoattractants for many immune cells, including neutrophils. Antagonism of CXCR2 that mobilizes neutrophil and monocyte from the bone marrow, neutrophil elastase inhibitors, and inhibition of G-CSF (granulocyte colony-stimulating factor), IL-23, and IL-17 that promote neutrophil survival are also options (*46*). Anti–IL-6, IL-1RA, and anti–TNF-α agents are already being investigated for COVID-19 treatment and are relevant to neutrophils, which express the requisite cytokine receptors. Furthermore, Janus kinase (JAK) inhibitors are currently in clinical trials and may also reduce neutrophil levels (*47*). Targeting toxic products of neutrophils such as S100A1/A2, HMGB1, and free radicals, but also the formation of NETs, could be beneficial (*21*).

In summary, this is a key longitudinal study immune profiling patients with COVID-19, which places equal emphasis on innate and adaptive immunity. We identify substantial alterations in the myeloid compartment in patients with COVID-19 that have not previously been reported. It would appear that comparable innate immune features have been evident in past pandemics with similar or even different viruses, and so, focusing immunomodulation strategies on neutrophils and monocytes is an urgent priority.

MATERIALS AND METHODS

Study design

Between 29 March and 7 May 2020, adults requiring hospital admission with suspected COVID-19 were recruited from four hospitals in the Greater Manchester area. Our research objective was to undertake an observational study to (i) examine the kinetics of the immune response in patients with COVID-19 and (ii) identify early indicators of disease severity. Informed consent was obtained for each patient. Peripheral blood samples were collected at Manchester University Foundation Trust (MFT), Salford Royal NHS Foundation Trust (SRFT), and Pennine Acute NHS Trust (PAT) under the framework of the Manchester Allergy, Respiratory and Thoracic Surgery (ManARTS) Biobank (study no. M2020-88) for MFT or the Northern Care Alliance Research Collection (NCARC) tissue biobank (study no. NCA-009) for SRFT and PAT (REC reference 15/NW/0409 for ManARTS and 18/WA/0368 for NCARC). Clinical information was extracted from written/electronic medical records. Patients were included if they tested positive for SARS-CoV-2 by RT-PCR on NP/oropharyngeal swabs or sputum. Patients with negative NP RT-PCR results were also included if there was a high clinical suspicion of COVID-19, the radiological findings supported the diagnosis, and there was no other explanation for symptoms. Patients were excluded if an alternative diagnosis was reached, where indeterminate imaging findings were combined with negative SARS-CoV-2 NP test or there was another confounding acute illness not directly related to COVID-19. The severity of disease was scored each day, based on degree of respiratory failure (Fig. 1B). Patients were not stratified for disease severity if there were no available clinical observation data or patients were recruited more than 7 days after hospital admission. Where severity of disease changed during admission, the highest disease severity score was selected for classification. The first available time point was used for all cross-sectional comparisons between mild, moderate, and severe disease. Peripheral blood samples were collected as soon after admission as possible and at 1- to 2-day intervals thereafter. For longitudinal analysis, we elected to correlate clinical data with immune parameters directly, rather than using the World Health Organization (WHO) ordinal scale on account of the small range of values this affords our inpatient cohort, which our study would not be powered to discern. Healthy blood samples were obtained from frontline workers at Manchester University and NHS Trusts (age range, 28 to 69 years; median age, 44.5 years; 42.5% males). Samples from healthy donors were examined alongside patient samples.

Isolation of PBMCs and serum

Whole venous blood was collected in tubes containing EDTA or serum gel clotting activator (Sarstedt). PBMCs were isolated by density gradient centrifugation using Ficoll-Paque Plus (GE Healthcare) and 50-ml SepMate tubes (STEMCELL Technologies) according to the manufacturer's protocol. Serum was separated by centrifuging serum tubes at 2000*g* at 4°C for 20 min.

Whole blood lysis

Red blood cell lysis was carried out using 10× volume of distilled water for 10 s followed by addition of 10× phosphate-buffered saline (PBS) to reestablish a 1× PBS solution and stop lysis. Cells were centrifuged at 500*g* for 5 min, and lysis was repeated if necessary.

Flow cytometry

White blood cells from lysed whole blood and isolated PBMCs separated by density gradient centrifugation were stained immediately on receipt. The following antibodies were used: BDCA-2 (clone 201A), CCR7 (clone G043H7), CD11b (clone ICRF44), CD11c (clone 3.9 or Bu15), CD123 (clone 6H6), CD14 (clone 63D3), CD16 (clone 3G8), CD19 (clone H1B19), CD24 (clone M1/69 or ML5), CD27 (clone M-T271), CD3 (clone OKT3 or UCHT1), CD38 (clone HIT2), CD4 (clone SK3), CD45 (clone 2D1), CD45RA (clone HI100), CD56 (clone MEM-188), CD62L (clone DREG-56), CD8 (clone SK1), HLA-DR (clone L234), ICOS (clone C398.4A), IgD (clone IA6-2), IgM (clone MHM-88), IgG (clone M1310G05), Ki-67 (clone Ki-67 or 11F6), PD-1 (clone EH12.2H7), perforin (clone dG9), CD66b (clone G10F5), CD64 (clone 10.1), IL-1β (clone H1b-98), and TNF-α (clone MAb11), all from BioLegend, and COX-2 (clone AS67) from BD Biosciences. PBMCs were also stimulated in vitro for 3 hours with LPS (10 ng/ml) in the presence of brefeldin A (10 μg/ml) to allow accumulation and analysis of intracellular proteins by flow cytometry. Cells were cultured in RPMI containing 10% fetal calf serum, L-glutamine, nonessential amino acids, Hepes, and penicillin-streptomycin (Gibco). For surface stains, samples were fixed with BD Cytofix (BD Biosciences) before acquisition, and for intracellular stains (Ki-67, COX-2, TNF-α, and IL-1β), the Foxp3/Transcription Factor Staining Buffer Set (eBioscience) was used. All samples were acquired on an LSRFortessa flow cytometer (BD Biosciences) and analyzed using FlowJo (TreeStar).

LEGENDplex

Thirteen different mediators associated with antiviral responses were measured in serum using LEGENDplex assays (BioLegend, San Diego, USA) according to the manufacturer's instructions.

Statistics

Results are presented as individual data points with medians. Statistical analysis was performed using Prism 8 Software (GraphPad). Normality tests were performed on all datasets. Groups were compared using an unpaired *t* test (normal distribution) or Mann-Whitney test (failing normality testing) for healthy individuals versus patients with COVID-19. Paired *t* test (normal distribution) or Wilcoxon matched-pairs signed-rank test (failing normality testing) was used for longitudinal data, where first and last time points were examined. One-way analysis of variance (ANOVA) with Holm-Sidak post hoc testing (normal distribution) or Kruskal-Wallis test with Dunn's post hoc testing (failing normality testing) was used for multiple group comparisons. Correlations were assessed with Pearson correlation coefficient (normal distribution) or Spearman's rank correlation coefficient test (failing normality testing) for separate parameters within the COVID-19 patient group. Information on tests used is detailed in figure legends. In all cases, a P value of ≤ 0.05 was considered significant. ns, not significant; $^{*}P < 0.05$, $^{**}P < 0.01$, $^{***}P < 0.001$.

SUPPLEMENTARY MATERIALS

immunology.sciencemag.org/cgi/content/full/5/51/eabd6197/DC1

Fig. S1. Immune cell types in patients with COVID-19.
Fig. S2. Serum cytokines and chemokines in patients with COVID-19.
Fig. S3. T cell activation in patients with COVID-19.
Fig. S4. B cell subsets in patients with COVID-19.
Fig. S5. Monocytes in patients with COVID-19.
Table S1. Raw data file (Excel spreadsheet).

View/request a protocol for this paper from *Bio-protocol*.

REFERENCES AND NOTES

1. M. Z. Tay, C. M. Poh, L. Rénia, P. A. MacAry, L. F. P. Ng, The trinity of COVID-19: Immunity, inflammation and intervention. *Nat. Rev. Immunol.* **20**, 363–374 (2020).
2. P. Zhou, X.-L. Yang, X.-G. Wang, B. Hu, L. Zhang, W. Zhang, H.-R. Si, Y. Zhu, B. Li, C.-L. Huang, H.-D. Chen, J. Chen, Y. Luo, H. Guo, R.-D. Jiang, M.-Q. Liu, Y. Chen, X.-R. Shen, X. Wang, X.-S. Zheng, K. Zhao, Q.-J. Chen, F. Deng, L.-L. Liu, B. Yan, F.-X. Zhan, Y.-Y. Wang, G.-F. Xiao, Z.-L. Shi, A pneumonia outbreak associated with a new coronavirus of probable bat origin. *Nature* **579**, 270–273 (2020).
3. S. Boettcher, M. G. Manz, Regulation of inflammation- and infection-driven hematopoiesis. *Trends Immunol.* **38**, 345–357 (2017).
4. P. Mehta, D. F. McAuley, M. Brown, E. Sanchez, R. S. Tattersall, J. J. Manson, COVID-19: Consider cytokine storm syndromes and immunosuppression. *Lancet* **395**, 1033–1034 (2020).
5. F. Wu, S. Zhao, B. Yu, Y.-M. Chen, W. Wang, Z.-G. Song, Y. Hu, Z.-W. Tao, J.-H. Tian, Y.-Y. Pei, M.-L. Yuan, Y.-L. Zhang, F.-H. Dai, Y. Liu, Q.-M. Wang, J.-J. Zheng, L. Xu, E. C. Holmes, Y.-Z. Zhang, A new coronavirus associated with human respiratory disease in China. *Nature* **579**, 265–269 (2020).
6. E. Terpos, I. Ntanasis-Stathopoulos, I. Elalamy, E. Kastritis, T. N. Sergentanis, M. Politou, T. Psaltopoulou, G. Gerotziafas, M. A. Dimopoulos, Hematological findings and complications of COVID-19. *Am. J. Hematol.* **95**, 834–847 (2020).
7. J. Fu, J. Kong, W. Wang, M. Wu, L. Yao, Z. Wang, J. Jin, D. Wu, X. Yu, The clinical implication of dynamic neutrophil to lymphocyte ratio and D-dimer in COVID-19: A retrospective study in Suzhou China. *Thromb. Res.* **192**, 3–8 (2020).
8. Y. Orr, J. M. Taylor, P. G. Bannon, C. Geczy, L. Kritharides, Circulating CD10-/CD16^{low} neutrophils provide a quantitative index of active bone marrow neutrophil release. *Br. J. Haematol.* **131**, 508–519 (2005).
9. J. Liu, Y. Liu, P. Xiang, L. Pu, H. Xiong, C. Li, M. Zhang, J. Tan, Y. Xu, R. Song, M. Song, L. Wang, W. Zhang, B. Han, L. Yang, X. Wang, G. Zhou, T. Zhang, B. Li, Y. Wang, Z. Chen, X. Wang, Neutrophil-to-lymphocyte ratio predicts critical illness patients with 2019 coronavirus disease in the early stage. *J. Transl. Med.* **18**, 206 (2020).
10. M. A. Smith, M. Hibino, B. A. Falcione; BCPS (AQ-ID), K. M. Eichinger, R. Patel, K. M. Empey, Immunosuppressive aspects of analgesics and sedatives used in mechanically ventilated patients: An underappreciated risk factor for the development of ventilator-associated pneumonia in critically ill patients. *Ann. Pharmacother.* **48**, 77–85 (2014).
11. S. Rinaldi, S. Pallikkuth, V. K. George, L. R. de Armas, R. Pahwa, C. M. Sanchez, M. F. Pallin, L. Pan, N. Cotugno, G. Dickinson, A. Rodriguez, M. Fischl, M. Alcaide, L. Gonzalez, P. Palma, S. Pahwa, Paradoxical aging in HIV: Immune senescence of B Cells is most prominent in young age. *Aging* **9**, 1307–1325 (2017).
12. E. J. Giamarellos-Bourboulis, M. G. Netea, N. Rovina, K. Akinosoglou, A. Antoniadou, N. Antonakos, G. Damoraki, T. Gkavogianni, M.-E. Adami, P. Katsaounou, M. Ntaganou, M. Kyriakopoulou, G. Dimopoulos, I. Koutsodimitropoulos, D. Velissaris, P. Koufargyris, A. Karageorgos, K. Katrini, A. Koutsoukou, Complex immune dysregulation in COVID-19 patients with severe respiratory failure. *Cell Host Microbe* **27**, 992–1000.e3 (2020).
13. M. Guilliams, A. Mildner, S. Yona, Developmental and functional heterogeneity of monocytes. *Immunity* **49**, 595–613 (2018).
14. M. Merad, J. C. Martin, Pathological inflammation in patients with COVID-19: A key role for monocytes and macrophages. *Nat. Rev. Immunol.* **20**, 355–362 (2020).
15. J. I. Kurland, R. Bockman, Prostaglandin E production by human blood monocytes and mouse peritoneal macrophages. *J. Exp. Med.* **147**, 952–957 (1978).
16. S. L. Cole, J. Dunning, W. L. Kok, K. H. Benam, A. Benlahrech, E. Repapi, F. O. Martinez, L. Drumright, T. J. Powell, M. Bennett, R. Elderfield, C. Thomas; MOSAIC investigators, T. Dong, J. M. Cauley, F. Y. Liew, S. Taylor, M. Zambon, W. Barclay, V. Cerundolo, P. J. Openshaw, A. J. McMichael, L.-P. Ho, M1-like monocytes are a major immunological determinant of severity in previously healthy adults with life-threatening influenza. *JCI Insight* **2**, e91868 (2017).
17. A. K. McElroy, R. S. Akondy, D. R. McIlwain, H. Chen, Z. Bjornson-Hooper, N. Mukherjee, A. K. Mehta, G. Nolan, S. T. Nichol, C. F. Spiropoulou, Immunologic timeline of Ebola virus disease and recovery in humans. *JCI Insight* **5**, e137260 (2020).
18. A. Grifoni, D. Weiskopf, S. I. Ramirez, J. Mateus, J. M. Dan, C. R. Moderbacher, S. A. Rawlings, A. Sutherland, L. Premkumar, R. S. Jadi, D. Marrama, A. M. de Silva, A. Frazier, A. F. Carlin, J. A. Greenbaum, B. Peters, F. Krammer, D. M. Smith, S. Crotty, A. Sette, Targets of T cell responses to SARS-CoV-2 coronavirus in humans with COVID-19 disease and unexposed individuals. *Cell* **181**, 1489–1501.e15 (2020).
19. V. Brinkmann, U. Reichard, C. Goosmann, B. Fauler, Y. Uhlemann, D. S. Weiss, Y. Weinrauch, A. Zychlinsky, Neutrophil extracellular traps kill bacteria. *Science* **303**, 1532–1535 (2004).
20. M. Ojima, N. Yamamoto, T. Hirose, S. Hamaguchi, O. Tasaki, T. Kojima, K. Tomono, H. Ogura, T. Shimazu, Serial change of neutrophil extracellular traps in tracheal aspirate of patients with acute respiratory distress syndrome: Report of three cases. *J. Intensive Care* **8**, 25 (2020).
21. B. J. Barnes, J. M. Adrover, A. Baxter-Stoltzfus, A. Borczuk, J. Cools-Lartigue, J. M. Crawford, J. Daßler-Plenker, P. Guerci, C. Huynh, J. S. Knight, M. Loda, M. R. Looney, F. M. Allister, R. Rayes, S. Renaud, S. Rousseau, S. Salvatore, R. E. Schwartz, J. D. Spicer, C. C. Yost, A. Weber, Y. Zuo, M. Egeblad, Targeting potential drivers of COVID-19: Neutrophil extracellular traps. *J. Exp. Med.* **217**, e20200652 (2020).
22. N. Chen, M. Zhou, X. Dong, J. Qu, F. Gong, Y. Han, Y. Qiu, J. Wang, Y. Liu, Y. Wei, J. Xia, T. Yu, X. Zhang, L. Zhang, Epidemiological and clinical characteristics of 99 cases of 2019 novel coronavirus pneumonia in Wuhan, China: A descriptive study. *Lancet* **395**, 507–513 (2020).
23. Y. Zuo, S. Yalavarthi, H. Shi, K. Gockman, M. Zuo, J. A. Madison, C. Blair, A. Weber, B. J. Barnes, M. Egeblad, R. J. Woods, Y. Kanthi, J. S. Knight, Neutrophil extracellular traps in COVID-19. *JCI Insight* **5**, e138999 (2020).
24. X. Yan, Q. Hao, Y. Mu, K. A. Timani, L. Ye, Y. Zhu, J. Wu, Nucleocapsid protein of SARS-CoV activates the expression of cyclooxygenase-2 by binding directly to regulatory elements for nuclear factor-kappa B and CCAAT/enhancer binding protein. *Int. J. Biochem. Cell Biol.* **38**, 1417–1428 (2006).
25. W. R. Coward, C. A. Feghali-Bostwick, G. Jenkins, A. J. Knox, L. Pang, A central role for G9a and EZH2 in the epigenetic silencing of cyclooxygenase-2 in idiopathic pulmonary fibrosis. *FASEB J.* **28**, 3183–3196 (2014).
26. C. Lucas, P. Wong, J. Klein, T. B. R. Castro, J. Silva, M. Sundaram, M. K. Ellingson, T. Mao, J. E. Oh, B. Israelow, T. Takahashi, M. Tokuyama, P. Lu, A. Venkataraman, A. Park, S. Mohanty, H. Wang, A. L. Wyllie, C. B. F. Vogels, R. Earnest, S. Lapidus, I. M. Ott, A. J. Moore, M. C. Muenker, J. B. Fournier, M. Campbell, C. D. Odio, A. Casanovas-Massana; Yale IMPACT Team, R. Herbst, A. C. Shaw, R. Medzhitov, W. L. Schulz, N. D. Grubaugh, C. D. Cruz, S. Farhadian, A. I. Ko, S. B. Omer, A. Iwasaki, Longitudinal analyses reveal immunological misfiring in severe COVID-19. *Nature* **584**, 463–469 (2020).
27. J. Hadjadj, N. Yatim, L. Barnabei, A. Corneau, J. Boussier, N. Smith, H. Péré, B. Charbit, V. Bondet, C. Chenevier-Gobeaux, P. Breillat, N. Carlier, R. Gauzit, C. Morbieu, F. Pène, N. Marin, N. Roche, T.-A. Szwebel, S. H. Merkling, J.-M. Treluyer, D. Veyer, L. Mouthon, C. Blanc, P.-L. Tharaux, F. Rozenberg, A. Fischer, D. Duffy, F. Rieux-Laucat, S. Kernéis, B. Terrier, Impaired type I interferon activity and inflammatory responses in severe COVID-19 patients. *Science* **369**, 718–724 (2020).
28. M. Liao, Y. Liu, J. Yuan, Y. Wen, G. Xu, J. Zhao, L. Cheng, J. Li, X. Wang, F. Wang, L. Liu, I. Amit, S. Zhang, Z. Zhang, Single-cell landscape of bronchoalveolar immune cells in patients with COVID-19. *Nat. Med.* **26**, 842–844 (2020).
29. Q. Ruan, K. Yang, W. Wang, L. Jiang, J. Song, Clinical predictors of mortality due to COVID-19 based on an analysis of data of 150 patients from Wuhan, China. *Intensive Care Med.* **46**, 846–848 (2020).
30. C. Huang, Y. Wang, X. Li, L. Ren, J. Zhao, Y. Hu, L. Zhang, G. Fan, J. Xu, X. Gu, Z. Cheng, T. Yu, J. Xia, Y. Wei, W. Wu, X. Xie, W. Yin, H. Li, M. Liu, Y. Xiao, H. Gao, L. Guo, J. Xie, G. Wang, R. Jiang, Z. Gao, Q. Jin, J. Wang, B. Cao, Clinical features of patients infected with 2019 novel coronavirus in Wuhan, China. *Lancet* **395**, 497–506 (2020).
31. C. Agostini, M. Facco, M. Siviero, D. Carollo, S. Galvan, A. M. Cattelan, R. Zambello, L. Trentin, G. Semenzato, CXC chemokines IP-10 and mig expression and direct migration of pulmonary CD8+/CXCR3+ T cells in the lungs of patients with HIV infection and T-cell alveolitis. *Am. J. Respir. Crit. Care Med.* **162**, 1466–1473 (2000).
32. J. Zhou, H. Chu, C. Li, B. H.-Y. Wong, Z.-S. Cheng, V. K.-M. Poon, T. Sun, C. C.-Y. Lau, K. K.-Y. Wong, J. Y.-W. Chan, J. F.-W. Chan, K. K.-W. To, K.-H. Chan, B.-J. Zheng, K.-Y. Yuen, Active replication of Middle East respiratory syndrome coronavirus and aberrant induction of inflammatory cytokines and chemokines in human macrophages: Implications for pathogenesis. *J. Infect. Dis.* **209**, 1331–1342 (2014).
33. K. K. W. To, I. F. N. Hung, I. W. S. Li, K.-L. Lee, C.-K. Koo, W.-W. Yan, R. Liu, K.-Y. Ho, K.-H. Chu, C.-L. Watt, W.-K. Luk, K.-Y. Lai, F.-L. Chow, T. Mok, T. Buckley, J. F. W. Chan, S. S. Y. Wong, B. Zheng, H. Chen, C. C. Y. Lau, H. Tse, V. C. C. Cheng, K.-H. Chan, K.-Y. Yuen, Delayed clearance of viral load and marked cytokine activation in severe cases of pandemic H1N1 2009 influenza virus infection. *Clin. Infect. Dis.* **50**, 850–859 (2010).
34. J. F. Bermejo-Martin, I. Martin-Loeches, J. Rello, A. Antón, R. Almansa, L. Xu, G. Lopez-Campos, T. Pumarola, L. Ran, P. Ramirez, D. Banner, D. C. Ng, L. Socias, A. Loza, D. Andaluz, E. Maravi, M. J. Gómez-Sánchez, M. Gordón, M. C. Gallegos, V. Fernandez, S. Aldunate, C. León, P. Merino, J. Blanco, F. Martin-Sanchez, L. Rico, D. Varillas, V. Iglesias, M. Á. Marcos, F. Gandía, F. Bobillo, B. Nogueira, S. Rojo, S. Resino, C. Castro, R. O. de Lejarazu, D. Kelvin, Host adaptive immunity deficiency in severe pandemic influenza. *Crit. Care* **14**, R167 (2010).
35. J. Liu, S. Li, J. Liu, B. Liang, X. Wang, H. Wang, W. Li, Q. Tong, J. Yi, L. Zhao, L. Xiong, C. Guo, J. Tian, J. Luo, J. Yao, R. Pang, H. Shen, C. Peng, T. Liu, Q. Zhang, J. Wu, L. Xu, S. Lu, B. Wang, Z. Weng, C. Han, H. Zhu, R. Zhou, H. Zhou, X. Chen, P. Ye, B. Zhu, L. Wang, W. Zhou, S. He, Y. He, S. Jie, P. Wei, J. Zhang, Y. Lu, W. Wang, L. Zhang, L. Li, F. Zhou, J. Wang, U. Dittmer, M. Lu, Y. Hu, D. Yang, X. Zheng, Longitudinal characteristics of lymphocyte responses and cytokine profiles in the peripheral blood of SARS-CoV-2 infected patients. *EBioMedicine* **55**, 102763 (2020).

36. F. A. Lagunas-Rangel, Neutrophil-to-lymphocyte ratio and lymphocyte-to-C-reactive protein ratio in patients with severe coronavirus disease 2019 (COVID-19): A meta-analysis. *J. Med. Virol.* **92**, 1733–1734 (2020).
37. C. Qin, L. Zhou, Z. Hu, S. Zhang, S. Yang, Y. Tao, C. Xie, K. Ma, K. Shang, W. Wang, D.-S. Tian, Dysregulation of immune response in patients with coronavirus 2019 (COVID-19) in Wuhan, China. *Clin. Infect. Dis.* **71**, 762–768 (2020).
38. G. Chen, D. Wu, W. Guo, Y. Cao, D. Huang, H. Wang, T. Wang, X. Zhang, H. Chen, H. Yu, X. Zhang, M. Zhang, S. Wu, J. Song, T. Chen, M. Han, S. Li, X. Luo, J. Zhao, Q. Ning, Clinical and immunological features of severe and moderate coronavirus disease 2019. *J. Clin. Invest.* **130**, 2620–2629 (2020).
39. A. G. Laing, A. Lorenc, I. D. M. Del Barrio, A. Das, M. Fish, L. Monin, M. Munoz-Ruiz, D. Mckenzie, T. Hayday, I. F. Quijorna, S. Kamdar, M. Joseph, D. Davies, R. Davis, A. Jennings, I. Zlatareva, P. Vantourout, Y. Wu, V. Sofra, F. Cano, M. Greco, E. Theodoridis, J. Freedman, S. Gee, J. N. En, Chan, S. Ryan, E. B. Blanco, P. Peterson, K. Kisand, L. Haljasmagi, L. Martinez, B. Merrick, K. Bisnauthsing, K. Brooks, M. Ibrahim, J. Mason, F. L. Gomez, K. Babalola, S. Abdul-Jawad, J. Cason, C. Mant, K. Doores, J. Seow, C. Graham, F. di Rosa, J. Edgeworth, M. S. Hari, A. Hayday, A consensus Covid-19 immune signature combines immuno-protection with discrete sepsis-like traits associated with poor prognosis. medRxiv 2020.06.08.20125112 (2020).
40. D. Mathew, J. R. Giles, A. E. Baxter, D. A. Oldridge, A. R. Greenplate, J. E. Wu, C. Alanio, L. Kuri-Cervantes, M. B. Pampena, K. D'Andrea, S. Manne, Z. Chen, Y. J. Huang, J. P. Reilly, A. R. Weisman, C. A. G. Ittner, O. Kuthuru, J. Dougherty, K. Nzingha, N. Han, J. Kim, A. Pattekar, E. C. Goodwin, E. M. Anderson, M. E. Weirick, S. Gouma, C. P. Arevalo, M. J. Bolton, F. Chen, S. F. Lacey, H. Ramage, S. Cherry, S. E. Hensley, S. A. Apostolidis, A. C. Huang, L. A. Vella; UPenn COVID Processing Unit, M. R. Betts, N. J. Meyer, E. J. Wherry, Deep immune profiling of COVID-19 patients reveals distinct immunotypes with therapeutic implications. *Science* **369**, eabc8511 (2020).
41. H.-Y. Zheng, M. Zhang, C.-X. Yang, N. Zhang, X.-C. Wang, X.-P. Yang, X.-Q. Dong, Y.-T. Zheng, Elevated exhaustion levels and reduced functional diversity of T cells in peripheral blood may predict severe progression in COVID-19 patients. *Cell. Mol. Immunol.* **17**, 541–543 (2020).
42. M. R. Woodruff, R. Ramonell, K. Cashman, D. Nguyen, A. Saini, N. Haddad, A. Ley, S. Kyu, J. C. Howell, T. Ozturk, S. Lee, W. Chen, J. Estrada, A. Morrison-Porter, A. Derrico, F. Anam, M. Sharma, H. Wu, S. Le, S. Jenks, C. M. Tipton, W. Hu, F. E.-H. Lee, I. Sanz, Dominant extrafollicular B cell responses in severe COVID-19 disease correlate with robust viral-specific antibody production but poor clinical outcomes. medRxiv 2020.04.29.20083717 (2020).
43. G. A. FitzGerald, Misguided drug advice for COVID-19. *Science* **367**, 1434 (2020).
44. T. H. Page, J. J. O. Turner, A. C. Brown, E. M. Timms, J. J. Inglis, F. M. Brennan, B. M. J. Foxwell, K. P. Ray, M. Feldmann, Nonsteroidal anti-inflammatory drugs increase TNF production in rheumatoid synovial membrane cultures and whole blood. *J. Immunol.* **185**, 3694–3701 (2010).
45. A. M. Risitano, D. C. Mastellos, M. Huber-Lang, D. Yancopoulou, C. Garlanda, F. Ciceri, J. D. Lambris, Complement as a target in COVID-19? *Nat. Rev. Immunol.* **20**, 343–344 (2020).
46. T. Németh, M. Sperandio, A. Mócsai, Neutrophils as emerging therapeutic targets. *Nat. Rev. Drug Discov.* **19**, 253–275 (2020).
47. J. J. O'Shea, D. M. Schwartz, A. V. Villarino, M. Gadina, I. B. McInnes, A. Laurence, The JAK-STAT pathway: Impact on human disease and therapeutic intervention. *Annu. Rev. Med.* **66**, 311–328 (2015).

Acknowledgments: This report is independent research supported by the North West Lung Centre Charity and National Institute for Health Research Clinical Research Facility at Manchester University NHS Foundation Trust. The views expressed in this publication are those of the author(s) and not necessarily those of the NHS, the North West Lung Centre Charity, National Institute for Health Research, or the Department of Health. We would like to acknowledge the Manchester Allergy, Respiratory and Thoracic Surgery Biobank, the Northern Care Alliance Research Collection tissue bank, and the North West Lung Centre Charity for supporting this project and thank the study participants for their contribution. A.S., T.F., P.D., and T.H. are supported by the NIHR Manchester Biomedical Research Centre. In addition, we would like to thank the Immunology community within the Lydia Becker Institute of Immunology and Inflammation, the core flow cytometry facility at University of Manchester, the Manchester COVID-19 Rapid Response Group, and the study participants for contribution. **Funding:** This work was supported by The Kennedy Trust for Rheumatology Research that provided a Rapid Response Award for costs associated with the laboratory analysis of the immune response in patients with COVID-19 to J.R.G., The Wellcome Trust (T.H., 202865/Z/16/Z; 106898/A/15/Z, which helped support some CIRCO members), The Wellcome Trust/Royal Society (E.R.M., 206206/Z/17/Z), the Lister Institute (J.E.K.), and BBSRC (J.E.K., BB/M025977/1; T.N.S., BB/S01103X/1). The Oxford and Manchester NIHR BRC provided support for study design and sample collection. **Author contributions:** E.R.M., M.M., S.B.K., J.E.K., C.J., T.N.S., J.R.G., and T.H. designed the study and performed tissue processing, data collection, data analysis, data interpretation, and manuscript writing. S.K. and M.R. performed data analysis and generated the figures. A.U., N.D.B., P.D., A.S., and T.F. performed sample collection and biobanking. A.U., A.S., and T.F. contributed to data interpretation, presentation of clinical data, and paper construction. L.-P.H., NIHR Respiratory TRC, G.M.L., CIRCO, and M.F. contributed to study design, patient consent and sample collection, and manuscript preparation. CIRCO performed tissue processing, data collection, and data analysis. **Competing interests:** G.M.L. is cofounder and scientific advisory board member of Gritstone Oncology Inc., which is a public company that develops therapeutic vaccines (primarily for the treatment of cancer). M.R. has a paid consultancy with AstraZeneca. The other authors declare that they have no competing interests. **Data and materials availability:** All data needed to evaluate the conclusions in the paper are present in the paper or the Supplementary Materials. Data and R code to reproduce the analysis are available at https://github.com/LydiaBecker.

The members of the NIHR Respiratory Translational Research Collaboration (TRC) collaborative group are Alex Horsley (Manchester BRC), Tim Harrison (Nottingham BRC), Joanna Porter (UCL BRC), Ratko Djukanovic (Southampton BRC), Stefan Marciniak (Cambridge BRC), Chris Brightling (Leicester BRC), Ling-Pei Ho (Oxford BRC), Lorcan McGarvey (Queen's University Belfast), and Jane Davies (Imperial BRC). The members of the CIRCO collaborative group are Rohan Ahmed, Halima Ali Shuwa, Miriam Avery, Katharine Birchall, Oliver Brand, Evelyn Charsley, Alistair Chenery, Christine Chew, Richard Clark, Emma Connolly, Karen Connolly, Simon Dawson, Laura Durrans, Hannah Durrington, Jasmine Egan, Claire Fox, Helen Francis, Miriam Franklin, Susannah Glasgow, Nicola Godfrey, Kathryn J. Gray, Seamus Grundy, Jacinta Guerin, Pamela Hackney, Mudassar Iqbal, Chantelle Hayes, Emma Hardy, Jade Harris, Anu John, Bethany Jolly, Verena Kästele, Saba Khan, Gabriella Lindergard, Sylvia Lui, Lesley Lowe, Alex G. Mathioudakis, Flora A. McClure, Joanne Mitchell, Clare Moizer, Katrina Moore, David J. Morgan, Stuart Moss, Syed Murtuza Baker, Rob Oliver, Grace Padden, Christina Parkinson, Laurence Pearmain, Mike Phuycharoen, Ananya Saha, Barbora Salcman, Nicholas A. Scott, Seema Sharma, Jane Shaw, Joanne Shaw, Elizabeth Shepley, Lara Smith, Simon Stephan, Ruth Stephens, Gael Tavernier, Rhys Tudge, Alison Uriel, Louis Wareing, Roanna Warren, Thomas Williams, Lisa Willmore, and Mehwish Younas.

Submitted 2 July 2020
Resubmitted 11 August 2020
Accepted 14 September 2020
Published First Release 17 September 2020
Final published 5 October 2020
10.1126/sciimmunol.abd6197

Citation: E. R. Mann, M. Menon, S. B. Knight, J. E. Konkel, C. Jagger, T. N. Shaw, S. Krishnan, M. Rattray, A. Ustianowski, N. D. Bakerly, P. Dark, G. M. Lord, A. Simpson, T. Felton, L.-P. Ho, NIHR Respiratory TRC, M. Feldmann, CIRCO, J. R. Grainger, T. Hussell, Longitudinal immune profiling reveals key myeloid signatures associated with COVID-19. *Sci. Immunol.* **5**, eabd6197 (2020).

Science Immunology

Longitudinal immune profiling reveals key myeloid signatures associated with COVID-19

Elizabeth R. Mann, Madhvi Menon, Sean Blandin Knight, Joanne E. Konkel, Christopher Jagger, Tovah N. Shaw, Siddharth Krishnan, Magnus Rattray, Andrew Ustianowski, Nawar Diar Bakerly, Paul Dark, Graham M. Lord, Angela Simpson, Timothy Felton, Ling-Pei Ho, NIHR Respiratory TRC, Marc Feldmann, CIRCO, John R. Grainger and Tracy Hussell

Sci. Immunol. **5**, eabd6197.
First published 17 September 2020
DOI: 10.1126/sciimmunol.abd6197

Myeloid upheaval in severe COVID-19

Severe COVID-19 disease is associated with immune hyperactivation accompanied by "cytokine storm." Mann *et al.* used longitudinal analysis of fresh blood samples from hospitalized COVID-19 patients to search for biomarkers that signal impending progression to severe disease. Several phenotypic and functional abnormalities of $CD14^+$ blood monocytes emerged as early-stage biomarkers predictive of increased severity of disease. Monocytes from patients with severe COVID-19 activated in vitro with lipopolysaccharide displayed increased proliferation and decreased expression of the prostaglandin-synthesizing cyclooxygenase-2 (COX-2) enzyme. Premature release of immature myeloid cells from the bone marrow contributes to innate immune dysfunction, causing more extensive lung damage and poorer clinical outcomes. These findings suggest that early treatment of COVID-19 targeting emergency myelopoiesis may help reduce the risk of subsequent clinical deterioration.

Science Immunology (ISSN 2470-9468) is published by the American Association for the Advancement of Science, 1200 New York Avenue NW, Washington, DC 20005. The title *Science Immunology* is a registered trademark of AAAS.